

Velocity of metal disks accelerated by explosions

Tomotaka Homae^{*†}, Kunihiko Wakabayashi^{**}, Tomoharu Matsumura^{**},
and Yoshio Nakayama^{**}

^{*}Toyama National College of Technology, 1-2 Ebie-neriya, Imizu, Toyama 933-0293, JAPAN
TEL : +81-766-86-5100

[†]Corresponding address : homae@nc-toyama.ac.jp

^{**}National Institute of Advanced Industrial Science and Technology (AIST),
Central 5, 1-1-1 Higashi, Tsukuba, Ibaraki 305-8565, JAPAN

Received : July 25, 2011 Accepted : December 20, 2011

Abstract

Explosives accelerate a surrounding layer of metal or other material by their detonation. In this study, stainless steel disks were accelerated by exploding composition C-4, weighing 40 g, in determining the flight velocity. The intention here was to identify the relationship between the ratio of the thickness of the disk to diameter (t/d), the standoff distance from the explosive material to the disk, and the flight velocity of the disk. The (t/d) was set to be 0.1, 0.2, 0.5, and 1.0. The same weight disks, being approximately 2.5 g, were used. The velocity increased with the cross sectional area of the disk. The velocity is substantially described by the momentum per unit cross section. The velocity decreased with standoff distance in the range from 0 mm to 38 mm. The velocity was basically constant within the range of 38 mm to 189 mm.

Keywords : explosive, fragment, velocity, metal disks, standoff distance.

1. Introduction

High explosives destroy and accelerate the materials surrounding the explosive material when they explode, and the accelerated material can impact and injure people or damage buildings. The damage caused by the accelerated materials can be extremely serious, thus making investigating the flight velocity of accelerated materials important. The velocity typically depends on a variety of factors that include the weight, cross section, density, shape of the material, degree to which the case seals in the explosive material, and the standoff distance between the explosive materials to the material accelerated.

The initial velocity of fragments from a warhead shell has been extensively studied in ensuring the most effective damage to the target. For example, the Gurney method¹⁾ is rather well-known. More recently, Zhang²⁾ proposed a theoretical computation method and compared it with experimental data on initial fragment velocity. The authors³⁾ carried out explosion tests using a steel container filled with TNT in thereby determining the flight velocity of the fragments. In an explosion of a 1 kg container filled with 1 kg of TNT the highest fragment

velocity was determined to be $1700 \pm 50 \text{ m}\cdot\text{s}^{-1}$ at a distance of $11.56 \pm 0.01 \text{ m}$ from the point of explosion. The effect of air resistance was also discussed.

Warheads are generally encased within a shell that the explosive comes in contact with. In addition, the explosive is completely covered by the shell. Part of the explosive energy is consumed in fragmentation of the shell, wherein the expansion of the explosion gases is confined by the fragments, and the fragments thus effectively accelerated. However, in industrial accidents any material, which did not cover the explosive material but was in contact with the explosive material or near the explosive materials, can result in damage. The explosion gases can freely expand in this situation, and hence the acceleration of the scattering material should differ from the case of warheads. The flight velocity of such scattering material is therefore fundamental data that can be used to suppress any damage to the surroundings, thus making examination of the velocity indispensable.

The authors⁴⁾ measured the velocity of a stainless steel disk accelerated by an explosion. The disk, with a diameter of 100 mm and a thickness of 20 mm was set in contact with 20 kg of composition C-4 explosive. The disk

simulated material that was in contact with but did not completely cover the explosive material. The experiment was carried out twice, with the average velocity of the disk, which flew 14.8 m, being $1213 \text{ m}\cdot\text{s}^{-1}$ and $1233 \text{ m}\cdot\text{s}^{-1}$. Hamashima⁵⁾ has also reported upon the velocity of stainless steel disks accelerated by exploding composition C-4. The weight of the composition C-4 used was 40 g and with a similar configuration to the above experiment. The standoff distance, described later, was set to be 0 mm, 10 mm, 20 mm, 30 mm, 40 mm, and 50 mm. The results were compared with numerical simulations using LS-DYNA. The velocity of the disk was approximately $1200 \text{ m}\cdot\text{s}^{-1}$ in the case of a standoff distance of 0 mm. The maximum standoff distance was limited to 50 mm and the shape of the disk fixed.

In this study, stainless steel disks were accelerated by the explosion of composition C-4 weighing 40 g in thereby determining their flight velocity. The intention was to identify the relationship between the ratio of the thickness of the disk to diameter (t/d), standoff distance from the explosive material to the disk, and the flight velocity of the disk.

2. Experimental

2.1 Test explosives

Composition C-4 explosive (Nippon Koki Co., Ltd.) was stuffed into Polymethyl methacrylate (PMMA) tubes of an internal diameter, thickness, and length of 34.0 mm, 2.0 mm, and 31.5 mm, respectively. 40 g of the explosive was used and the density adjusted to $1400 \text{ kg}\cdot\text{m}^{-3}$. Exploding-bridgewire (EBW) detonators (RP-501, Teledyne RISI, Inc.) were utilized. A digital delay and pulse generator (DG 535, Stanford Research Systems, Inc.) was used to send the precise appropriate delay pulses to the firing system (FS-43, Teledyne RISI, Inc.).

2.2 Disks

The disks, made of stainless steel (SUS304, a Japanese Industrial Standard), were prepared to simulate the scattered materials. The ratio of the thickness of the disk to the diameter (t/d) was set to be 0.1, 0.2, 0.5, and 1.0. The diameter and thickness of the four kinds of disks differed but the disks were all the same weight of approximately 2.5 g. The diameters were 16.4 mm, 12.6 mm, 9.3 mm, and 7.4 mm. The thicknesses were 1.5 mm, 2.5 mm, 4.6 mm, and 7.4 mm.

2.3 Standoff distance

Figure 1 shows the configuration of the explosive in the PMMA tubes and the disks. The standoff distance was defined to be from the face of the explosive to the face of the disk. The standoff distance was set to be 0 mm, 12.7 mm, 38.0 mm, 88.2 mm, and 189.1 mm. In the 0 mm case the disk was in close contact with the explosive. The corresponding Hopkinson scaled distance⁶⁾ was $0 \text{ m}\cdot\text{kg}^{-1/3}$, $0.037 \text{ m}\cdot\text{kg}^{-1/3}$, $0.111 \text{ m}\cdot\text{kg}^{-1/3}$, $0.258 \text{ m}\cdot\text{kg}^{-1/3}$, and $0.553 \text{ m}\cdot\text{kg}^{-1/3}$, respectively. A PMMA tube of an internal diameter and thickness of 34.0 mm and 2.0 mm, respectively, was used to set the standoff distance. This tube will hereinafter be referred to as the spacer tube. A spacer tube suits being used to set the accurate standoff distance, but it confines the air blast and can thus affect the velocity of the disk. As many holes as possible were therefore drilled in the tube to suppress the confinement. This spacer tube will be hereinafter referred to as the spacer tube with holes. The diameter of the holes was either 9 mm or 11 mm. The ratio of the overall area of the holes to the lateral area of the spacer tube is tabulated in Table 1. In addition, PMMA tubes without holes were also tested as spacer tubes in thereby evaluating the effect of the tubes on the flight velocity.

Thread was stretched at the opposite side of the spacer

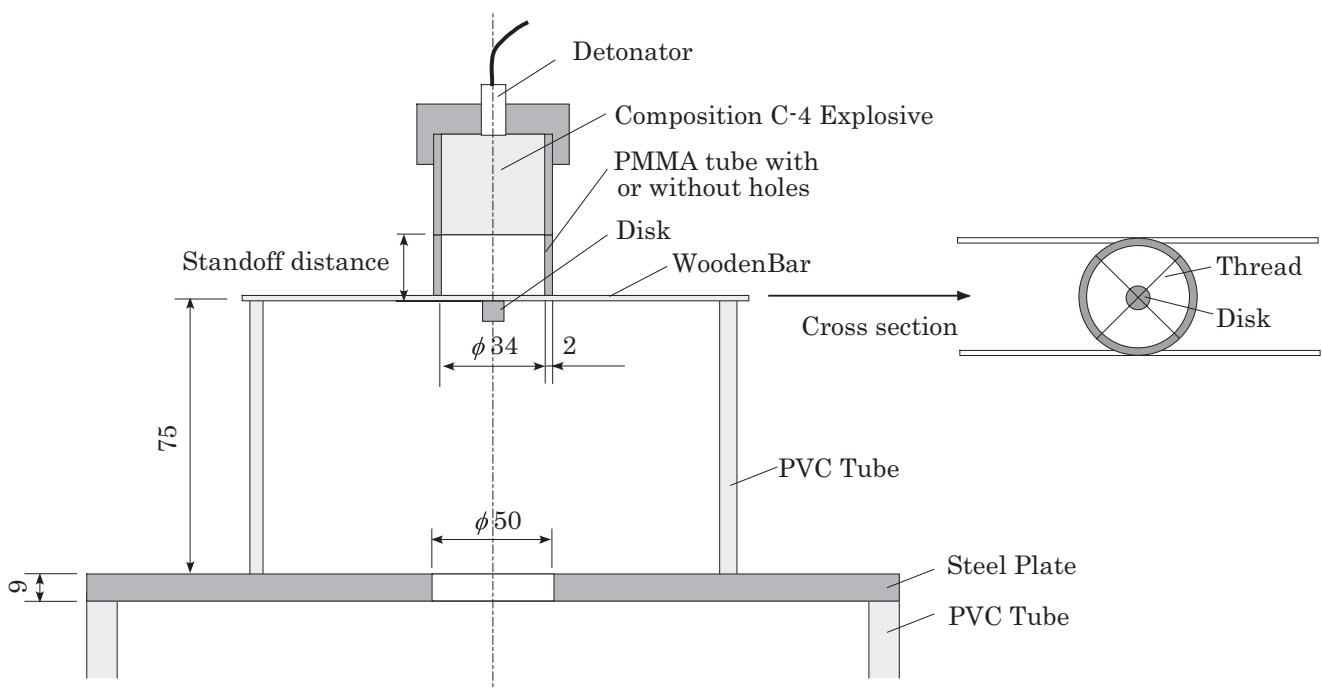


Figure 1 Configuration of explosive and metal disks used in this study.

Table 1 Holes in PMMA tube.

Length [mm]	Diameter of Holes [mm]	Number of Holes	Areal Ratio of Holes to PMMA Pipe [%]
189.1	11	104	41.6
88.2	11	48	41.2
38.0	9	24	32.0
12.7	9	8	31.9

tube to the explosive. The thread was made of polyester of a diameter of approximately 0.1 mm. The disk was bonded to the thread with epoxy resin. The end face of the disk and the explosive faced each other.

The disk was placed in the direction of the detonation in this study. Held⁷⁻⁹⁾ reported the blast impulse in this direction to be the largest. The configuration used in this study resulted in the fastest velocity of the disk.

2.4 Velocity measurement

Figure 2 shows the configuration of the apparatus used to measure the flight velocity. The experiments took place at atmospheric pressure. The disks flew from top to bottom within a large polyvinyl chloride (PVC) tube of a length, internal diameter, and thickness of 1100 mm, 247 mm, and 10 mm, respectively. The tube had vents for the explosion gases and openings to record images, and is shown in Figure 2. A steel plate was fixed at the top of the PVC tube. The steel plate was used to restrain the bright explosion gases that could have obstructed the velocity being measured by the high-speed camera. The steel plate was square, with sides 267 mm long, and the thickness of the plate was 9 mm. A circular opening with a diameter of 50 mm was prepared in the center of the plate to allow passage of the disk. Preliminary advance experiments demonstrated that the opening diameter of 50 mm did not affect the velocity of the disk but was enough to restrain the bright explosion gases generated. The explosive and the disk were fixed to two thin wooden bars of a length, thickness, and width of 200 mm, 4 mm, and 4 mm, respectively, and then placed on a PVC tube of a length, internal diameter, and thickness of 75 mm, 146 mm, and 10 mm, respectively.

The velocity of the disk was then measured using a high-speed video camera (HPV-1, Shimadzu Corporation). Images were recorded during a flight of 500 mm from 630 mm from the initial position. The time interval of the frames was 16 μs or 32 μs. The digital delay and pulse generator, described above, sent the appropriate delay pulse to the camera to start recording. 105 mm f/2.5 or 135 mm f/2 lenses were employed. A flash (Matsushita Electric Industrial Co. Ltd PE-560 MGN or Panasonic Photo & Lighting Co. Ltd PE-60 SG) was used as the light source.

3. Results and discussion

Figure 3 (a)–(c) shows a typical image taken by the high-speed camera. The obtained images were clear enough to analyze the velocity in almost experiments. Some of the disks rotated as they flew. As shown in Figure 3 (c) the case of a standoff distance of 0 mm resulted in the disks being destroyed and the small fragments recorded, excluding a (t/d) of 0.1, although the disk was not destroyed in the experiments in reference 4) and 5) that took place in similar conditions. In the experiments the disks were all made of the same regulated stainless steel, and hence the strength of the hardening due to work must have affected the fragmentation.

The position of the disk in each image was determined in thus obtaining the relationship between time and displacement. The velocity of the disk was then determined based on linear fitting of that relationship. The coefficient of determination was approximately 0.999. After taking into account the air resistance the relationship between the velocity of the disk and the distance is expressed using eq. (1)^{3,10)}.

$$v(R) = v_0 \cdot \exp \left[- \left(\frac{C_d \cdot \rho \cdot A}{2m} \right) \cdot R \right] \tag{1}$$

where $v(R)$ is the velocity at distance R , v_0 the initial velocity, ρ the density of air, A the cross section of the disk, m the mass of the disk, and C_d the drag coefficient.

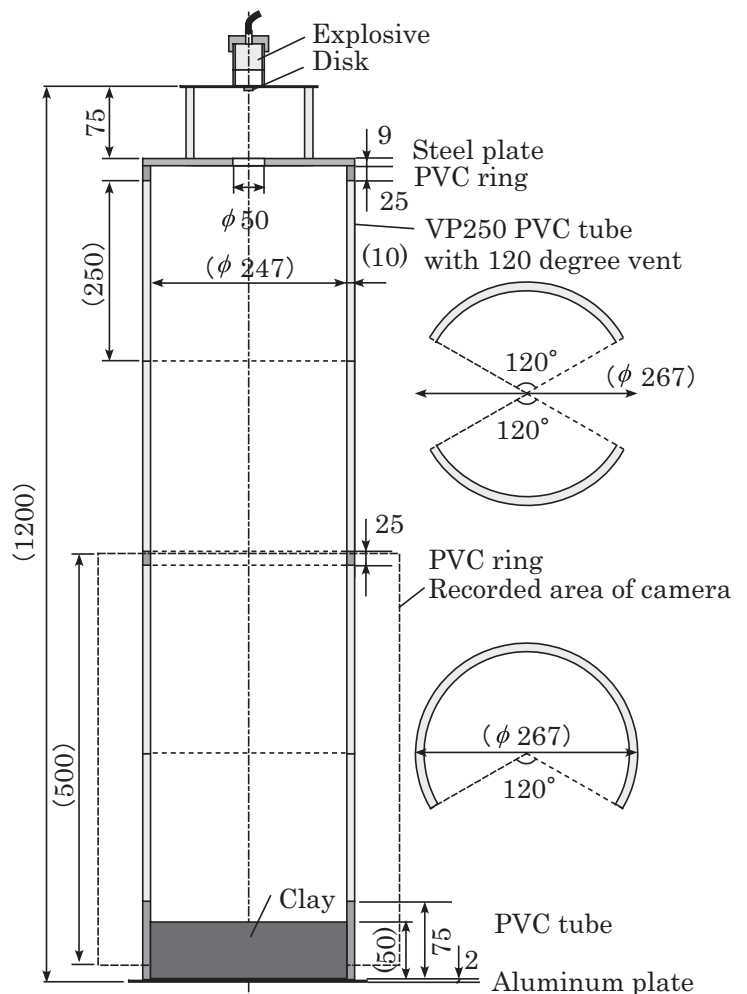


Figure 2 Configuration of flight velocity measurement apparatus.

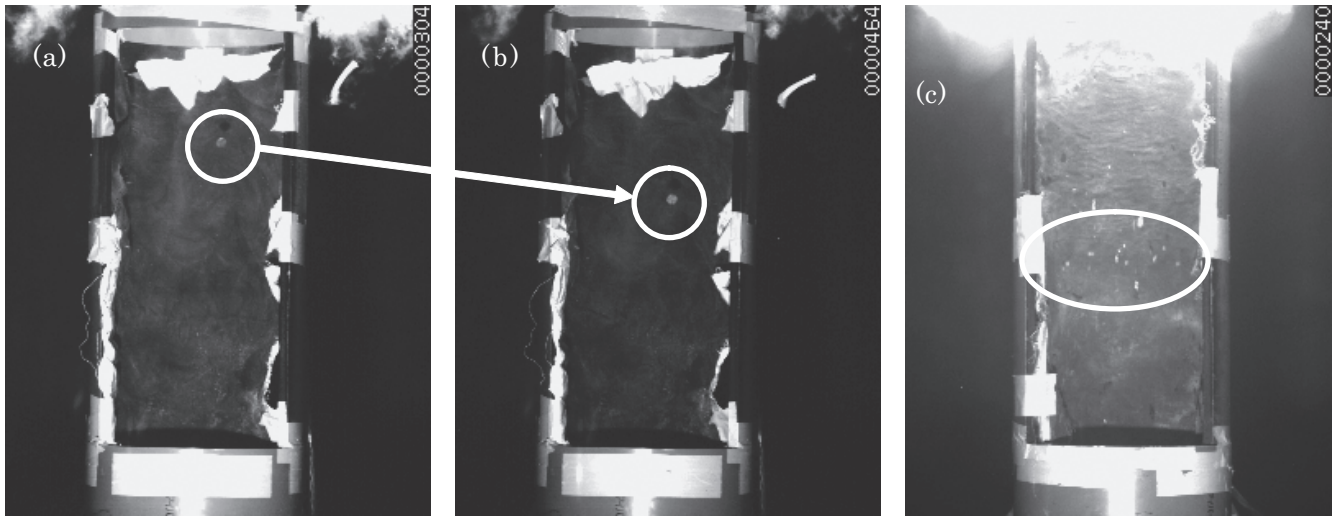


Figure 3 Typical images taken by high-speed camera. (a), (b) Images taken in experiment No.9. (t/d) of 0.2 and standoff distance of 88.2 mm. (b) was recorded 160 μ s after (a). The white circles emphasize the movement of the disk. The disk rotated as it flew. (c) Images taken in experiment No.6. (t/d) of 0.2 and standoff distance of 0 mm. Fragments can be observed within the white ellipse.

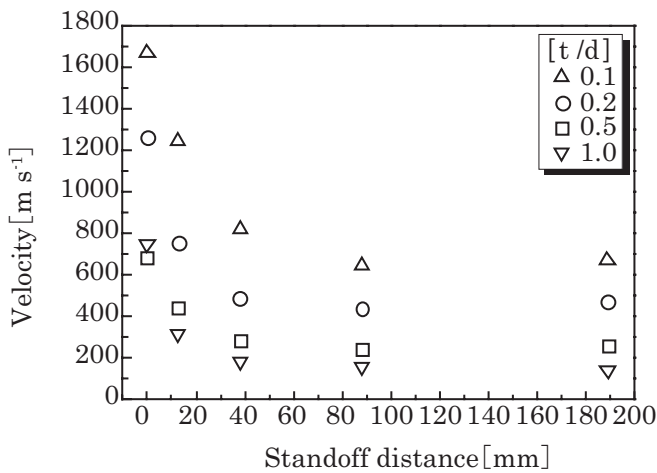


Figure 4 Relationship between standoff distance and velocity.

To estimate the effect of the air resistance the drag coefficient of the disk and the initial velocity were presumed to be 1.2 and 1200 $\text{m}\cdot\text{s}^{-1}$, respectively. The density of the air was $1.2\text{ kg}\cdot\text{m}^{-3}$. Substituting these values into eq. (1) resulted in the velocity after a flight of 500 mm, which is the length of the area recorded by the high-speed camera, being calculated to be 1179 $\text{m}\cdot\text{s}^{-1}$. The decrease in velocity was 1.8%. The disk was therefore regarded to move at constant velocity. As in the fragmentation experiments the velocity was determined using a fragment, which can be traced on all the images, the significance of the velocity in such experiments differed from the others. The determined velocity and corresponding experimental conditions are tabulated in Table 2. The determined velocity is in accordance with the velocity in references 4) and 5).

The velocity obtained with the spacer tubes with holes is represented in Figures 4 and 5. Figure 4 demonstrates the velocity to be basically constant and only dependent on (t/d) when the standoff distance was more than 38 mm. Figure 5 shows that the velocity generally decreased with (t/d).

Table 2 Velocity of disks and corresponding experimental conditions.

Number	t/d	Standoff distance [mm]	Scaled Standoff Distance [$\text{m kg}^{-1/3}$]	Holes on spacer	Velocity [m/s]
1	0.1	0.0	0.000	Yes	1669
2	0.1	12.7	0.037	Yes	1241
3	0.1	38.0	0.111	Yes	821
4	0.1	88.3	0.258	Yes	644
5	0.1	189.0	0.553	Yes	671
6	0.2	0.0	0.000	Yes	1259*
7	0.2	12.7	0.037	Yes	752
8	0.2	38.0	0.111	Yes	484
9	0.2	88.2	0.258	Yes	436
10	0.2	189.0	0.553	Yes	473
11	0.5	0.0	0.000	Yes	681*
12	0.5	12.7	0.037	Yes	442
13	0.5	38.0	0.111	Yes	285
14	0.5	88.2	0.258	Yes	242
15	0.5	189.1	0.553	Yes	260
16	1.0	0.0	0.000	Yes	750*
17	1.0	12.7	0.037	Yes	310
18	1.0	38.0	0.111	Yes	155
19	1.0	88.1	0.258	Yes	158
20	1.0	189.1	0.553	Yes	138
21	0.1	12.7	0.037	No	1238
22	0.1	38.0	0.111	No	824
23	0.1	88.1	0.258	No	703
24	0.1	188.8	0.552	No	713
25	0.2	12.7	0.037	No	743
26	0.2	38.0	0.111	No	501
27	0.2	88.1	0.258	No	397
28	0.2	188.9	0.552	No	475

*The case of a standoff distance of 0 mm resulted in the disks being destroyed, excluding (t/d) of 0.1. The velocity shown in this table is the representative velocity of fragments.

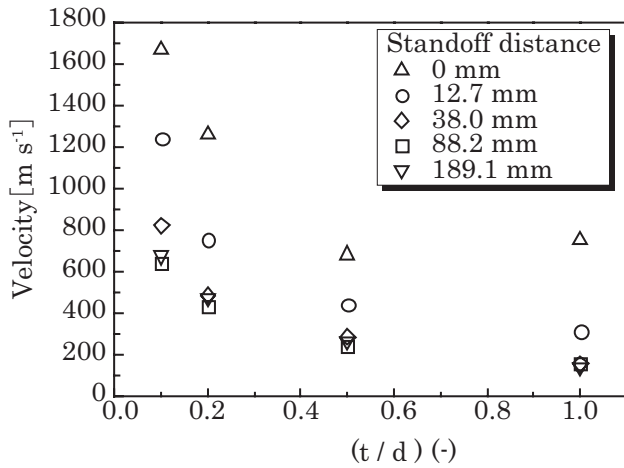


Figure 5 Relationship between (t/d) and velocity.

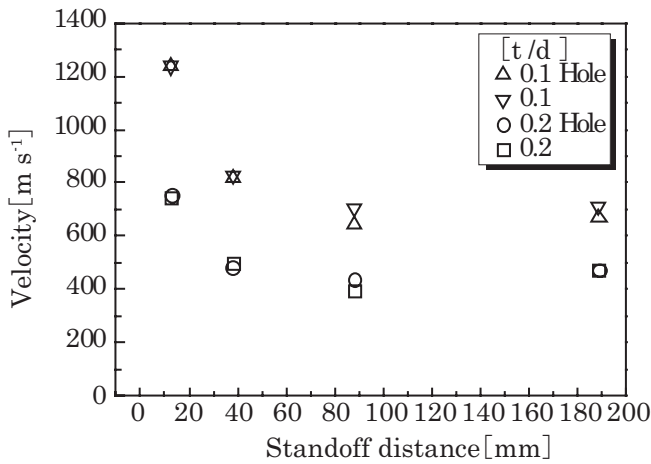


Figure 6 Effect of holes on PMMA tubes.

The effect of the holes on the spacer tube is examined in Figure 6. The difference is not at all obvious and the effect of the holes ambiguous. The holes in the spacer tube, whose areal ratio was from 30% to 40%, did not affect the velocity of the disk.

The relationship between the velocity and the standoff distance, as shown in Figure 4, demonstrates the velocity to strongly depend on the (t/d) at the same standoff distance. The velocity of the disk should therefore be related to the impulse caused by the explosion. The impulse per unit cross section of the disk must be same at the same standoff distance. The amount of the impulse should be proportionate to the cross section of the disk. The momentum, as described by eq. (2), should be proportionate to the impulse.

$$p = mv \tag{2}$$

where p is the momentum of the disk, m the mass of the disk, and v the velocity measured in this study. The four kinds of disks used in this study had basically the same m but different cross sections. Based on the above, therefore, the momentum per unit cross section c in eqs. (3) and (4) should not depend on the (t/d).

$$c = \frac{p}{A} \tag{3}$$

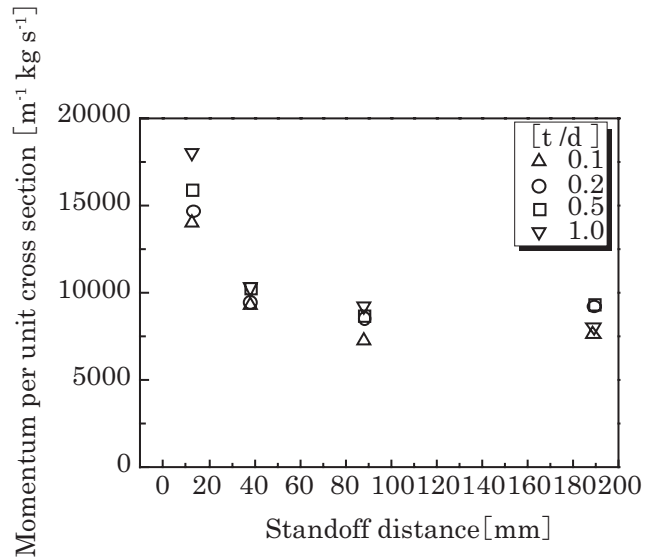


Figure 7 Relationship between standoff distance and momentum per unit cross section.

$$c = \frac{Amv}{\pi d^2} \tag{4}$$

where A is the cross section and d the diameter of the disk. As the disk was fragmented the data from a standoff distance 0mm was eliminated. Figure 7 shows the relationship between the standoff distance and the momentum per unit cross section. The difference due to (t/d) at same standoff distance was up to 20%, which is small when compared with Figure 4. The velocity therefore can be substantially described using the momentum per unit cross section. Similar to the velocity (Figure 4) the momentum per unit cross section did not strongly depend on the standoff distance in the case of being more than 38 mm.

Held⁹⁾ reported the impulse per unit area around cylindrical explosive (TNT/HMX (30/70)) to be 0.77 kg. The precise impulses from the figure in the paper were rather difficult to determine, but impulse per unit area at 0.28 m·kg^{-1/3}, 0.55 m·kg^{-1/3} was approximately 1.5×10⁴ m⁻¹ · kg·s⁻¹. The momentum in this study was smaller than that of Held but comparable. Held⁹⁾ also reported that the impulse definitely decreased at 0.82 m·kg^{-1/3} and 1.09 m·kg^{-1/3}. The explosion of spherical explosives normally results in the reflected blast impulse decreasing with distance¹¹⁾. The cylindrical shape of the explosive used in this study should have affected the constant momentum when larger than 38 mm, although the confinement due to the spacer tube could not be excluded.

The results demonstrate that the velocity of material accelerated by an explosion can be estimated using the standoff distance, weight, and cross section of the material. Any dependence on shape and density of the material will be a future subject of research.

4. Conclusion

This study examined the flight velocity of metal disks accelerated by explosions. Summarized conclusions follow.

1. The flight velocity of a disk accelerated by an explosion depended on the cross section of the disks of the same weight and at the same standoff distance (Figure 5). The velocity could be significantly described using the momentum per unit cross section (Figure 7).

2. The flight velocity decreased at standoff distances of 0 mm to 38.0 mm but then basically remained constant when greater than 38 mm (Figure 4).

3. A PMMA spacer tube was used make the standoff-distance more accurate. Tubes with holes and without holes had no obvious difference in velocity. The ratio of the hole to lateral area of the spacer tube was 30–40 % (Figure 6).

The dependence on the kind of explosive, shape, and density of the material will be a future subject of research. This study will be used in a technique for measuring the impulse at a very near point to the explosion.

Acknowledgement

This study was conducted as part of the commissioned project of “Technical Standards Examination for Mitigation of Damage from Explosions” by the Nuclear and Industrial Safety Agency of the Ministry of Economy, Trade and Industry of Japan in FY2008.

References

- 1) R.W. Gurney, Ballistic Research Laboratory Report No. 405, Aberdeen Proving Ground, Maryland (1943).
- 2) Q. Zhang, C. Miao, D. Lin, and C. Bai, *Int. J. Impact Eng.*, 28, 1129 (2003).
- 3) K. Wakabayashi, T. Homae, K. Ishikawa, E. Kuroda, T. Matsumura, and Y. Nakayama, *Sci. Tech. Energetic Materials*, 70, 94 (2009).
- 4) Unpublished data.
- 5) H. Hamashima, S. Kubota, T. Saburi, and Y. Ogata, *Mat. Sci. Forum*, 673, 301 (2011).
- 6) W.E. Baker, “Explosions in Air”, Univ. of Texas Press, Austin, Texas (1973).
- 7) M. Held, *Propellants, Explosives, Pyrotechnics*, 24, 17 (1999).
- 8) M. Held, *Propellants, Explosives, Pyrotechnics*, 26, 290 (2001).
- 9) M. Held, *Propellants, Explosives, Pyrotechnics*, 27, 279 (2002).
- 10) “Manual of NATO safety principles for the storage of military ammunition and explosives AASTP-1 Edition1”, II -5-34, NATO Group of Experts of the Safety Aspects for Transportation and Storage of Military Ammunition and Explosives (2006).
- 11) W.E. Baker, P.A. Cox, P.S. Westine, J.J. Kulesz, and R.A. Strehlow, “Explosion Hazards and Evaluation”, Elsevier (1983).

爆薬の爆発により加速される金属円板の速度

保前友高^{*†}, 若林邦彦^{**}, 松村知治^{**}, 中山良男^{**}

爆発物が爆発すると、周囲に存在する物体は加速されて飛散物となる。本研究では、飛散物速度の評価を行うため、飛散物の模擬物としてステンレス製円板を使用した実験を行った。特に、円板の厚さ・直径の比 (t/d)、爆薬と円板の距離 (Standoff distance) と速度の関係に着目した評価を行った。 (t/d) については、ほぼ同じ質量の円板で比較したところ、断面積が大きいほど、速度も大きかった。速度は、おおむね、単位断面積当たりの運動量で整理できた。爆薬と円板の距離については、爆薬がコンポジションC-4 40gの場合、0 mmから38 mmまでの範囲では、距離が大きくなるに伴い、速度が小さくなったが、38 mmから189 mmの範囲では、ほぼ一定であった。

*富山高等専門学校 商船学科 〒933-0293 富山県射水市海老江練合1-2
TEL: 0766-86-5100

†Corresponding address: homae@nc-toyama.ac.jp

**独立行政法人 産業技術総合研究所 安全科学研究部門 〒305-8565 茨城県つくば市東1-1-1 中央第5